

Time Domain Channel Model for the THz Band

Kazuhiro Tsujimura, Kenta Umebayashi*, Joonas Kokkonen†, and Janne Lehtomäki†

* Tokyo University of Agriculture and Technology, Koganei-shi, Tokyo

† Centre for Wireless Communications (CWC), Oulu, Finland

Abstract—Impulse response is proposed for wireless nanosensor networks which is used the terahertz band (THz band: 0.1–10 THz) and short range (1–100 cm). There is not only a line-of-sight (LoS) path but also a reflected path in nanosensor networks. In THz band, rough surface on the reflector significantly effect due to very short wavelength. This paper focuses on frequency domain and time domain channel models and, for wireless communication analysis the impulse response is very important specially. Frequency domain channel model represents molecular absorption and rough surface effect which are unique in THz band. And time domain channel model shows delayed wave even in LoS path. Reflected path has significantly strong effect to received signal from LoS path at long distance between transmitter and receiver than at short distance, relatively. These channel model leads to development of THz band communication technique.

Index Terms—Causality, channel models, impulse response, molecular absorption, reflected path, terahertz band

I. INTRODUCTION

Envisioned applications for nanodevices include health monitoring, plants monitoring, haptic interfaces, interconnected offices, damage detection systems, and ultra-high-speed on-chip communication [1], [2]. For a nanodevice to be capable of reporting sensing information or receiving tasks, communication between devices is required [1]. Electromagnetic (EM) communication and molecular communication have been proposed to enable device-to-device communication in wireless nanosensor networks (WNSNs) [1].

One of the suggested frequency bands for nanodevices is the terahertz band (0.1–10 THz) [3], which is our frequency of interest. In contrast to the UHF band, the effect of molecular absorption needs to be considered in the THz band [3]. Molecular absorption and its impact on transmittance of the channel were studied in [3]. Transmittance is the ratio of received signal power to transmitted signal power in the channel for frequency domain and is modeled with the Beer-Lambert law. Then, the molecular absorption loss in the THz channel is derived by the Beer-Lambert law [3]. Molecular absorption is decided by the composition of a medium, relative humidity (RH), pressure, and temperature, significantly. The signal in THz band experiences frequency selective fading.

Time domain channel model is come from the transmittance in [4]–[6]. [4] took into account of molecular absorption and antenna response and they proposed Time Spread On-Off Keying (TS-OOK) for both of single and multi user. [5] focused on not only molecular absorption but also a particle scattering which comes from aerosols such as water droplet, and their link was assumed as a line-of-sight (LoS). Our

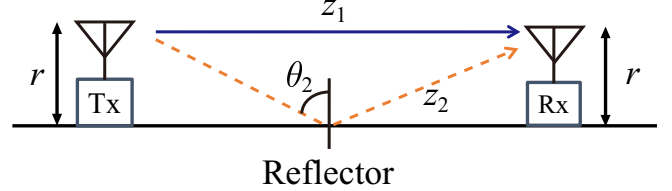


Fig. 1. Multipath scenario ($M = 2$) with LoS and reflected path. ©2019 IEEE. Reprinted, with permission, from IEEE Transaction on Terahertz Science and Technology.

previous research in [6] focused on impulse response as a time domain channel model by considering causality.

In this paper, at first we show a derivation of an impulse response as the channel model by a transmittance information. Next, several example of time impulse responses are shown.

II. FREQUENCY DOMAIN CHANNEL MODEL FOR WNSN

There may be multiple paths in WNSN, such as LoS path and reflected paths in [7]. So we assume two path model in which one path is LoS and the other path is reflected path like in Fig. 1. In this multipath, the parameters are as follows: $n_i = 1$, $r = 1$ cm, and $z_1 = 1$ –100 cm. Spreading loss and molecular absorption are considered in the LoS path in [4]. The reflected path should be taken into account roughness of reflector surface. For a simple channel model between a transmitter and a receiver, antenna characteristics are not considered in this paper. The frequency response of the multipath channel $H(f)$ is defined by

$$H(f) = \sum_{m=1}^M H_m(f, z_m), \quad (1)$$

where f , z_m , and $H_m(f, z_m)$ are the frequency, the distance of the m th path, and the frequency response of the m th path, respectively. The frequency response $H_1(f, z_1) = H_{1,\text{los}}(f, z_1)$ corresponds to the LoS path and $H_m(f, z_m) = H_{m,\text{refl}}(f, z_m)$ for $m \neq 1$ corresponds to the m th reflected path.

A. LoS path model

The distance between the transmitter and the receiver is set to z_1 cm. The transmittance $|H_1(f, z_1)|^2$ is defined by

$$|H_1(f, z_1)|^2 = \frac{P(f, z_1)}{P(f, z=0)}, \quad (2)$$

where f is the frequency, $P(f, z=0)$ represents the transmitted signal power, $P(f, z_1)$ is the received signal power and

$H_1(f, z_1)$ is the frequency response. The path loss is given by the transmittance as [3]

$$\text{Path loss [dB]} = -10\log_{10}(|H_1(f, z_1)|^2). \quad (3)$$

As can be seen in (2), the transmittance contains the amplitude component of the frequency response, but not the phase component. By considering the spreading loss and the molecular absorption loss, the transmittance (2) can be calculated as [3]

$$|H_1(f, z_1)|^2 = [A_{abs}(f, z_1) \times A_{spread}(z_1)]^{-1}, \quad (4)$$

where $A_{spread}(z_1)$ is the spreading loss and $A_{abs}(f, z_1)$ is the molecular absorption loss. The spreading loss in a LoS link for an ideal isotropic transmitter is $A_{spread}(z_1) = 4\pi z_1^2$. The molecular absorption loss $A_{abs}(f, z_1)$ can be described by the line absorption loss $A_{la}(f, z_1)$ and the continuum absorption loss $A_{ca}(f, z_1)$ as [8]

$$A_{abs}(f, z_1) = A_{la}(f, z_1) \times A_{ca}(f, z_1). \quad (5)$$

with $A_{la}(f, z_1)$ and $A_{ca}(f, z_1)$ given by

$$\begin{aligned} A_{la}(f, z_1) &= \exp\left(\sum_i k_{la}^i(f) z_1\right) \\ A_{ca}(f, z_1) &= \exp\left(\sum_j k_{ca}^j(f) z_1\right), \end{aligned} \quad (6)$$

where i and j are indices for molecular species and the source of the continuum absorption, respectively, and k_{la} and k_{ca} are the line absorption coefficient and the continuum absorption coefficient, respectively.

Fig. 2 shows the path loss caused by the spreading loss and the molecular absorption loss in the THz band as a function of distance and frequency. The parameters used in this figure are as follows: the distance range from 1 cm to 100 cm, pressure $p = 1010$ hPa, RH = 69.6% and temperature $T = 298.55$ K. To better show the details of the path loss, values greater than 80 dB are suppressed to 80 dB. The molecular absorption is occurred at specific frequency so we can see frequency selective fading in LoS path in Fig. 2.

B. Reflected path model

The power spectrum $|H_{m,\text{refl}}(f, z_m)|^2$ of the reflected path is given by

$$|H_{m,\text{refl}}(f, z_m)|^2 = |H_{m,\text{los}}(f, z_m) \cdot R(f)|^2, \quad (7)$$

where $H_{m,\text{los}}(f, z_m)$ and $R(f)$ are the frequency response of the m th path for the LoS path and the reflection coefficient, respectively. According to Kirchhoff's theory, the reflection coefficient $R(f)$ for a rough surface is given by

$$R(f) = \gamma(f) \cdot \rho(f), \quad (8)$$

where $\gamma(f)$ is the smooth surface reflection coefficient from the Fresnel equation for the electromagnetic (EM) wave and $\rho(f)$ is the Rayleigh roughness factor. $\gamma(f)$ is the total Fresnel equation of both of the perpendicular and parallel components $\gamma(f) = \gamma_{\perp}(f) + \gamma_{\parallel}(f)$. The smooth surface

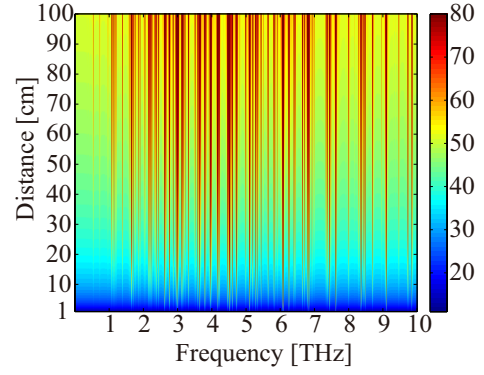


Fig. 2. Path loss due to spreading loss and molecular absorption in the THz band in the distance range from 1 cm to 100 cm. Pressure $p = 1010$ hPa, RH = 69.6% and temperature $T = 298.55$ K.

reflection coefficient for the perpendicular component $\gamma_{\perp}(f)$ is described by

$$\gamma_{\perp}(f) = \frac{n_i \cos \theta_m - n_t \sqrt{1 - \left(\frac{n_i}{n_t} \sin \theta_m\right)^2}}{n_i \cos \theta_m + n_t \sqrt{1 - \left(\frac{n_i}{n_t} \sin \theta_m\right)^2}}, \quad (9)$$

where n_i , n_t and θ_m are the refractive index of the air, the reflector and incident angle of m th path, respectively [10]. Without loss of generality, reflection coefficient for the parallel component $\gamma_{\parallel}(f)$ can be obtained by a similar approach. The refractive index of the reflector n_t is frequency dependent. But so is n_i , actually. The rough surface effect is characterized by the Rayleigh roughness factor $\rho(f)$ as

$$\rho(f) = \exp\left(-\frac{8\pi \cdot f^2 \cdot \sigma^2 \cdot \cos^2 \theta_m}{c^2}\right). \quad (10)$$

We assume that the height of the rough surface has a Gaussian distribution with standard deviation σ . This assumption is valid for many indoor building materials [11].

III. TIME DOMAIN CHANNEL MODEL

Our methodology obtains the phase component from the transmittance which is amplitude component. Specifically, the method employs the Hilbert transform to obtain the phase component leading to a physically valid impulse response. The received signal $y(t)$ at time t can be obtained by the convolution between the transmitted signal $x(t)$ and the impulse response, $h(\tau, z)$, as

$$y(t) = \int_{-\infty}^{\infty} h(\tau, z) x(t - \tau) d\tau. \quad (11)$$

The causal impulse response satisfies

$$h_{\text{causal}}(\tau, z) = \begin{cases} h_{\text{causal}}(\tau, z) & \tau \geq \tau_p \\ 0 & \tau < \tau_p, \end{cases} \quad (12)$$

where τ_p is the propagation delay. The frequency response of $h_{\text{causal}}(\tau, z)$ is given by

$$H(f, z) = e^{-j2\pi f \tau_p} \int_0^\infty h_{\text{causal}}(\tau + \tau_p, z) e^{-j2\pi f \tau} d\tau. \quad (13)$$

$H'(f, z)$ is defined as *causal frequency response* in this paper and is defined by

$$H'(f, z) = \int_0^\infty h_{\text{causal}}(\tau + \tau_p, z) e^{-j2\pi f \tau} d\tau, \quad (14)$$

which leads to $H(f, z) = e^{-j2\pi f \tau_p} H'(f, z)$. Let $\exp[-\alpha(f, z)]$ and $\phi(f, z)$ denote the amplitude and phase components of $H'(f, z)$, respectively, i.e., $\exp[-\alpha(f, z)] = |H'(f, z)| = |H(f, z)|$ and $\phi(f, z) = \arg(H'(f, z))$. Then, $H'(f, z)$ for LoS path is given by [8], [12]

$$H'(f, z) = \exp[-\alpha(f, z) + j\phi(f, z)], \quad (15)$$

and $H'(f, z)$ for reflected paths is

$$H'(f, z) = \exp[-\alpha(f, z) + j(\phi(f, z) + \pi)]. \quad (16)$$

Since the impulse response satisfies causality, $\alpha(f, z)$ and $\phi(f, z)$ are Hilbert transform pairs [8], [12]. Therefore, $\phi(f, z)$ is given by

$$\phi(f, z) = \frac{1}{\pi} \text{PV} \int_{-\infty}^\infty \frac{\alpha(f', z)}{f - f'} df', \quad (17)$$

where PV represents Cauchy principal value [13]. Given $|H(f, z)|$, $H(f, z)$ is available based on (13)–(17). Finally, the causal impulse response is given by

$$h_{\text{causal}}(\tau, z) = \mathcal{F}^{-1}[H(f, z)]. \quad (18)$$

Finally, frequency band in THz band for multipath is get by band pass filter (BPF). In BPF scenario, the impulse response $h^{\text{FB}}(\tau)$ can be obtained by

$$h^{\text{FB}}(\tau, f_c) = \int_{-\infty}^\infty h_{\text{causal}}(\tau') h_{rc}(\tau - \tau', B, f_c) d\tau'. \quad (19)$$

where B is the transmission band, and f_c is the center frequency and $h_{rc}(\tau, B, f_c)$ represents the effect of the BPFs. We employ root raised cosine filters as the BPF at both transmitter and receiver. B and f_c determine the frequency band.

IV. CHARACTERISTIC OF THE IMPULSE RESPONSE

In this section, we discuss characteristic of the impulse response in terms of distance, multipath, and frequency band.

First, we focus on the impulse response in the LoS path at $z_1 = 10$ cm and 80 cm in Figs. 3 and 4. As increasing distance, the impact of delayed wave is also increasing which come from frequency selective fading in THz band.

Impulse responses of multipath at $z_1 = 10$ cm and 80 cm are in Figs. 5 and 6. The time 0 in these figures means the arrival time of the first wave and the arrival time of the reflected wave is 6.6 ps and 0.8 ps in Figs. 5 and 6, respectively. We can see that first wave at $z_1 = 80$ cm is small than at $z_1 = 10$ cm. As

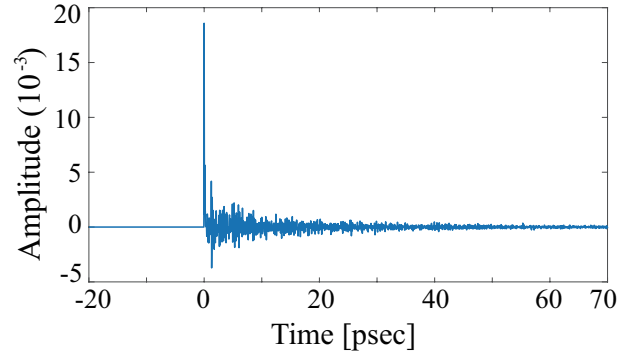


Fig. 3. Impulse response for LoS path in $z_1 = 10$ cm. Pressure $p = 1010$ hPa, RH = 69.6%, and temperature $T = 298.55$ K.

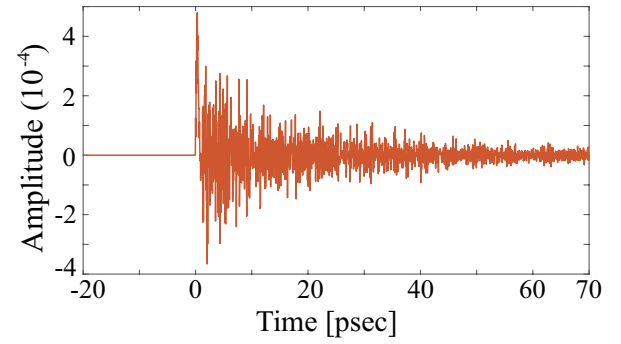


Fig. 4. Impulse response for LoS path in $z_1 = 80$ cm. Pressure $p = 1010$ hPa, RH = 69.6%, and temperature $T = 298.55$ K.

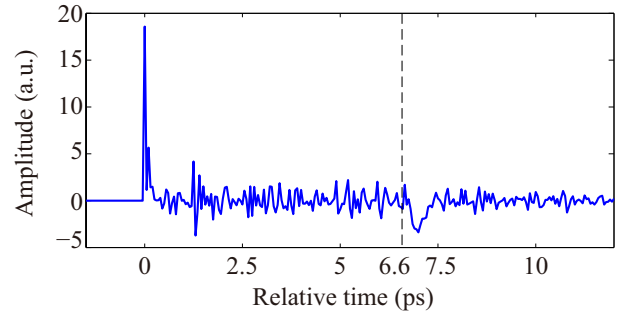


Fig. 5. Impulse response for multipath environment in $z_1 = 10$ cm. Pressure $p = 1010$ hPa, RH = 69.6%, and temperature $T = 298.55$ K. ©2019 IEEE. Reprinted, with permission, from IEEE Transaction on Terahertz Science and Technology.

z_1 is increasing, spreading loss and molecular absorption loss in both of LoS path and reflected path are increasing. Still, the impact of reflected wave to LoS path at $z_1 = 80$ cm is stronger than $z_1 = 10$ cm, relatively.

In Fig. 7 and 8, the impulse response for frequency band whose bandwidth $B = 0.3$ THz for multipath at $z_1 = 10$ cm at $f_c = 0.3$ THz and 7.15 THz, respectively. (a) in both of figures are the impulse response for LoS path and (b) are the impulse response for multipath. At 0.3 THz the impulse response has strong delayed response than LoS path. However, at 7.15 THz, the difference of impulse response between multipath and LoS

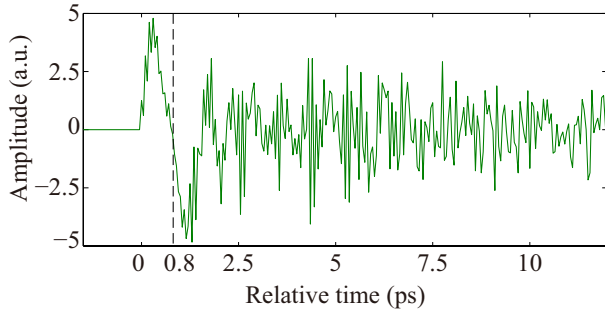


Fig. 6. Impulse response for multipath environment in $z_1 = 80$ cm. Pressure $p = 1010$ hPa, RH = 69.6%, and temperature $T = 298.55$ K. ©2019 IEEE. Reprinted, with permission, from IEEE Transaction on Terahertz Science and Technology.

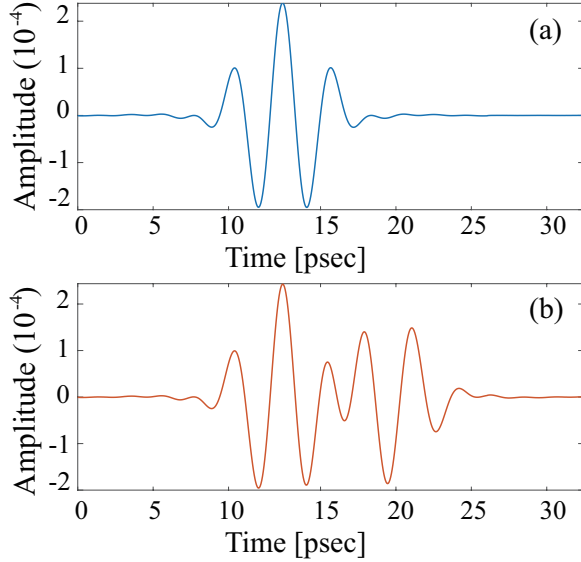


Fig. 7. (a) Impulse response for frequency band $B = 0.3$ THz for LoS path in $z_1 = 10$ cm at $f_c = 0.3$ THz. (b) Impulse response for frequency band $B = 0.3$ THz for multipath in $z_1 = 10$ cm at $f_c = 0.3$ THz. Pressure $p = 1010$ hPa, RH = 69.6%, and temperature $T = 298.55$ K.

path is negligible. It is multipath fading which comes from the reflected wave.

V. CONCLUSION

This paper introduced the causal impulse response as a time domain channel model in the THz band. We explained both of frequency domain and time domain channel model for THz band. We can see frequency selective fading by molecular absorption in THz band in LoS. At $z_1 = 80$ cm, reflected path has remarkable effect to LoS path. Additionally, frequency band results show us necessary to select proper band for THz communication.

ACKNOWLEDGMENT

The work of Joonas Kokkonen and Janne Lehtomäki under TERRANOVA project has received funding from Horizon 2020, European Union's Framework Programme for Research and Innovation, under grant agreement No. 761794.

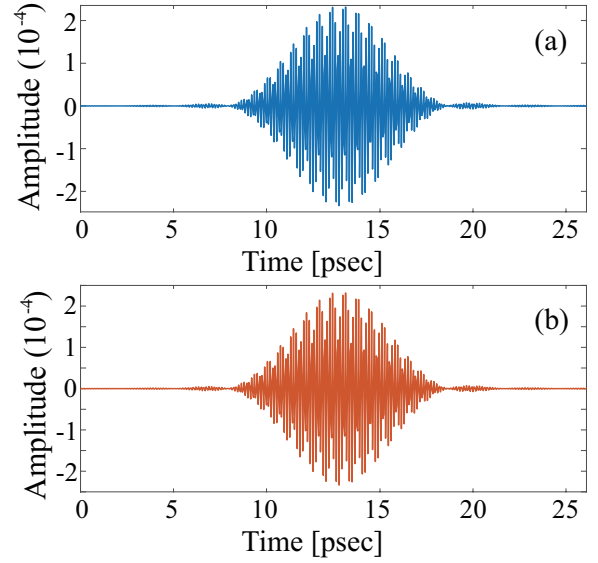


Fig. 8. (a) Impulse response for frequency band $B = 0.3$ THz for LoS path in $z_1 = 10$ cm at $f_c = 7.15$ THz. (b) Impulse response for frequency band $B = 0.3$ THz for multipath in $z_1 = 10$ cm at $f_c = 7.15$ THz. Pressure $p = 1010$ hPa, RH = 69.6%, and temperature $T = 298.55$ K.

REFERENCES

- [1] I. F. Akyildiz and J. M. Jornet, "Electromagnetic wireless nanosensor-networks," *Nano Communication Networks*, vol. 1, no. 1, pp. 3–19, Mar 2010.
- [2] I. F. Akyildiz, J. M. Jornet, and C. Han, "Terahertz band: Next frontier for wireless communications," *Physical Communication*, vol. 12, pp. 16–32, Sep 2014.
- [3] J. M. Jornet and I. F. Akyildiz, "Channel modeling and capacity analysis for electromagnetic wireless nanonetworks in the terahertz band," *IEEE Transactions on Wireless Communications*, vol. 10, no. 10, pp. 3211–3221, Oct 2011.
- [4] J. Kokkonen, J. Lehtomäki, K. Umehayashi, and M. Juntti, "Frequency and time domain channel models for nanonetworks in terahertz band," *IEEE Transactions on Antennas and Propagation*, vol. 63, no. 2, pp. 678–691, Feb 2015.
- [5] J. M. Jornet and I. F. Akyildiz, "Femtosecond-long pulse-based modulation for terahertz band communication in nanonetworks," *IEEE Transactions on Communications*, vol. 62, no. 5, pp. 1742–1754, May 2014.
- [6] K. Tsujimura, K. Umehayashi, J. Kokkonen, J. Lehtomäki, and Y. Suzuki, "A causal channel model for thz band," *IEEE Transaction on THz science and technology*, vol. 8, no. 1, pp. 52–62, Jan. 2018.
- [7] C. Han, A. O. Bicen, and I. F. Akyildiz, "Multi ray channel modeling and wideband characterization for wireless communications in the terahertz band," *IEEE Transactions on Wireless Communications*, vol. 14, no. 5, pp. 2402–2412, May 2015.
- [8] S. Paine, "The am atmospheric model," Smithsonian Astrophysical Observatory, SMA Technical Memo 152, Feb 2012.
- [9] L. S. Rothman, I. E. Gordon, A. Barbe *et al.*, "The HITRAN 2008 molecular spectroscopic database," *Journal of Quantitative Spectroscopy and Radiative Transfer*, vol. 110, no. 9–10, pp. 533–572, Jun–July 2009.
- [10] S. J. Adams, *Electromagnetic theory*. McGraw-Hill BookCompany, 1941.
- [11] C. Jansen *et al.*, "Diffuse scattering from rough surfaces in thz communication channels," *IEEE Transactions on Terahertz Science and Technology*, vol. 1, no. 2, pp. 462–472, Nov. 2011.
- [12] H. Kuzmany, *Solid-State Spectroscopy*. Springer, 1998.
- [13] I. S. Gradshteyn and I. M. Ryzhik, *Tables of integrals Series and Products*, 7th ed. Academic Press, 1992.
- [14] B. Sklar, *Digital Communications: Fundamentals and Applications*, 2nd ed. Prentice Hall, 2001.